Article:
Sun, C, Wang, L, Wang, Z et al. (4 more authors) (2015) Finite Element Analysis of A Retrieved Custom-Made Knee Prosthesis. Journal of Mechanics in Medicine and Biology, 15 (3). 1550020. pp. 1550020-1550034. ISSN 0219-5194

https://doi.org/10.1142/S0219519415500207

FINITE ELEMENT ANALYSIS OF A RETRIEVED CUSTOM-MADE KNEE PROSTHESIS

ChangNing Sun*, Ling Wang*,‡,¶, Zhen Wang†,§,¶, Lei Geng†, DiChen Li*, Miao Sui£, ZhongMin Jin*

*State Key Laboratory for Manufacturing Systems Engineering, Xi'an Jiaotong University
Xi'an, 710049, People's Republic of China

‡menlwang@mail.xjtu.edu.cn

†Department of Orthopaedics, Xijing Hospital, the Fourth Military Medical University
Xi'an, 710032,People's Republic of China

§wangzhen@fmmu.edu.cn

£State Agencies Drug Clinical Trials, the 210th Hospital of PLA
DaLian, 116021,People's Republic of China

Custom-made knee prostheses have been widely used to reconstruct the function of the lower limb in bone tumor resections. A custom-made tumor knee prosthesis was retrieved on account of prosthesis loosening post-surgery. Misalignment between the anatomical axis of the femur and the axis of the femoral stem as well as the material loss at the posterior region of the tibial plateau were considered to be the primary causes of the failure. Based on this hypothesis, finite element analysis was performed to investigate the contact mechanics of the prosthesis while implanted in vivo. The maximum deformation at the femur was 0.59 mm and 1.17 mm when the misalignment angle was 3° and 6°, respectively. Besides, the maximum contact pressure at the tibial plateau was 44.88 MPa at an extremely high flexion of angle 135° during squatting or kneeling. Uneven stress distribution at the femur, which came from the misalignment, was the main cause of loosening, which was aggravated indirectly with the material loss at the posterior region of the tibial plateau. Optimized prosthesis design and appropriate selection, with accurate surgical positioning and targeted rehabilitation training programme are important considerations for prolonging life-span of prostheses in vivo.

Keywords: Knee prosthesis; finite element analysis; misalignment; aseptic loosening.

1. Introduction

Total knee arthroplasty (TKA) is commonly used to preserve joint function in limb sparing surgery for malignant bone tumors around the knee joint. Custom-made

¶Corresponding authors[1]

knee prostheses have been widely used for TKA since 1980s.[1,2] However, the failure rate of tumor knee prostheses is still unsatisfactory. Complications such as deep infection, aseptic loosening and mechanical failure are in a dominate position.[3,4] Additionally, once the prostheses failed, a revision surgery must be performed to salvage the limb. The difficulty and complexity of revision surgery is much higher than primary TKA, in which problems such as segmental bone defect, soft tissue coverage and poor post-operative function need to be solved.

For better understanding of the failure mechanisms and the optimization of the prosthesis design, previous researches have been mainly based on visual inspections. In clinical practice, the main adopted method is a combination of visual inspection on retrieved prostheses and Computed Tomography (CT) images. Blunn et al.[5] s-tudied the wear type of condylar knee prostheses from 280 retrievable samples, and found that delamination was the principal wear type. The causes of disassembly of a distal femur modular prosthesis were analyzed and reported by Galasso et al.,[6] mainly based on the CT images of the patient. Moreover, they inferred that the risk of disassembly might connect with the modularity. Nevertheless, the inaccuracy and the dependence on the experience of clinicians are main limitations of visual inspections. For further research of the failure mechanisms of prostheses such as wear and aseptic loosening, a variety of observation facilities have been employed. Oliveira et al.[7] investigated the failure mechanism which led to the fracture in the medial portion of the baseplate from a retrieved modular prosthesis. Design for the assembly of the tibial component was proved to be inefficient in this prosthesis. A fractographic analysis and a microstructural study of a fractured stem of a cementless hip prosthesis by Chao et al.[8] concluded that the fatigue process due to the stress concentration triggered the fracture of femoral neck of hip prosthesis. Similar conclusion was drawn by Rodriguez et al..[9] Optical microscope, scanning electronic microscopy and energy disperse spectroscopy were applied to determine the failure reason of the femoral stem in hip prosthesis. Various metallurgical tests of a high nitrogen stainless steel femoral stem in hip prosthesis were implemented by Poffey.[10] A failure analysis was presented by Liza et al.[11] to investigate the wear modes of an ultra-high molecular polyethylene (UHMWPE) tibial insert. Several of the observation methods were utilized in this research. However, mechanical problems, which are closely related to the mechanical environment in vivo, are the main failure reason of prostheses.[12,13]

Moreover, the structure of custom-made knee prosthesis is complicated, so it is difficult to acquire the underlying mechanism intuitively by observation. Therefore, finite element analysis (FEA) has been considered for retrieval studies. Previously, FEA has been widely used in biomechanics study of joint replacement implants and was accounted as a preclinical evaluation tool of artificial joint. A vast majority of research work was in the following three aspects: contact mechanics,[14,15] wear prediction[16,17] and fixation simulation on bone-prosthesis interface.[18] In addition, FEA was used in failure analysis of hip prosthesis by Graze et al..[19] Numerical simulation indicated that the premature fatigue failure of the femoral stem in hip prosthesis was enhanced by proximal loosening. Fonseca et al.[20] investigated a fractured prosthesis and concluded that overloading at the plate/stem transition zone caused the fracture by FEA. Besides, they suggested that appropriate assessment of bone mineralization should be emphasized again. But since the difficulty of modeling, FEA is seldom used in mechanical analysis of custom-made prosthesis.

The aim of this study was to investigate the mechanical failure mechanism of a custom-made knee prosthesis. And the main purpose of this study was to focus on the misalignment between the anatomical axis of the femur and the axis of the femoral stem of the prosthesis as well as the material loss at the tibial plateau. This was achieved in two parts: on one hand, the effect of the misalignment angle on the stress/ strain of the bone by three dimensional FEA with the assistance of reverse engineering techniques. On the other hand, contact mechanics study on the posterior region of the tibia plateau at high flexion was also carried out using FEA and Confocal Laser Scanning Microscope (CLSM).

2. Materials and methods

2.1. *Clinical Information*

A male patient, aged 39, weight of 69 Kg, was referred to the outpatient service of Xijing Hospital of Fourth Military Medical University because of postoperative recurrence of giant cell tumor of bone at left distal femur and was hospitalized in July, 2003. And the patient was treated with segmental resection and reconstruction with a custom-made biaxial hinge total knee prosthesis. CT image after the surgery is presented in Fig 1 (a). In 2012, a tumble resulted in leg length discrepancy, left lower limb being shorter than right lower limb by 10 cm. In April 2013, the

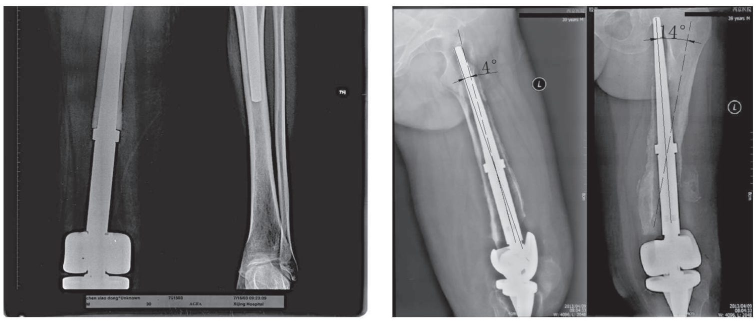

(a) (b)

Fig. 1. CT images of the patient: (a) After primary arthroplasty, (b) 10 years after primary arthroplasty, before revision arthroplasty. The dotted lines represent the anatomical axis of the femur while the solid lines represent the axis of the femoral stem.

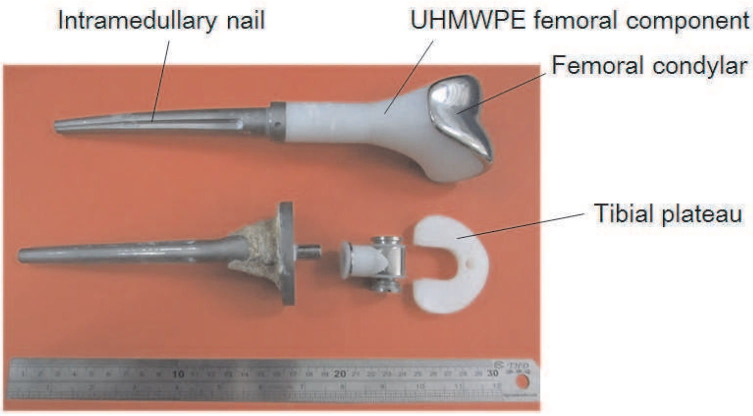

Fig. 2. Retrieved prosthesis showing the intramedullary nail, the femoral and the tibial parts.

patient was diagnosed as prosthesis loosening post-surgery and sinus forming. Then a revision arthroplasty was operated. The CT images before the revision surgery are presented in Fig 1 (b). The misalignment angle between the and the axis of the femoral stem in frontal plane was 14 ° while in cortical plane was 4 ° . The retrieved prosthesis in revision arthroplasty is presented in Fig 2. From CT images as shown in Fig 1, the misalignment angle was increased during prosthetic service. Moreover, serious material loss was observed at the posterior region of the tibial plateau as shown in Fig 3 (a) and the CLSM (OLS4000, OLYMPUS, Japan) image is presented in Fig 3 (b).

Based on the observations in Fig 1, misalignment between the anatomical axis of the femur and the axis of the femoral stem was found to increase, which worsened

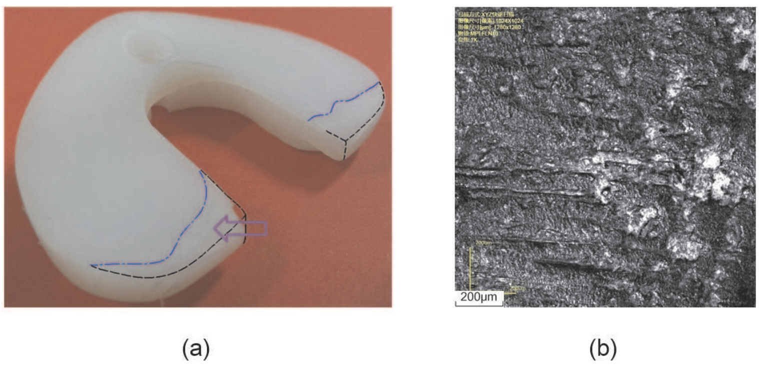

Fig. 3. (a) Retrieved tibial plateau; dashed line represented unworn outline of posterior region at tibial plateau. Dotted line represented boundary of worn area. (b) CLSM image taken on the surface of the posterior region at the tibial plateau (arrow).

the biomechanical condition of the prosthesis. Meanwhile, the collision between the UHMWPE tibial plateau and the UHMWPE femoral component was conjectured to be the primary cause of the material loss at the posterior region of the tibial plateau when the knee was under deep flexion.

2.2. *3D solid modeling*

Reverse engineering of artificial joints has been widely used in finite element analysis in order to obtain CAD models. First, the UHMWPE components of the prosthesis were scanned by micro-CT (Y. Cheetah, YXLON, Germany) while a laser scanner (Faro P12-7, Faro) was used for scanning the titanium alloy components. Mimics 10.01 (Materialise, Belgium) and Geomagic 12 (Geomagic, USA) were used to reconstruct 3D model from collected data. The femur was simplified as a hollow cylinder with 5 mm wall thickness which was determined from CT image of the patient. The void between the femur and the intramedullary nail was filled with bone cement. The assembled model of the whole prosthesis is presented in Fig 4.

Collision between the UHMWPE femoral component and the tibial plateau occurred when the flexion angle reached 135°. In order to investigate the effect of

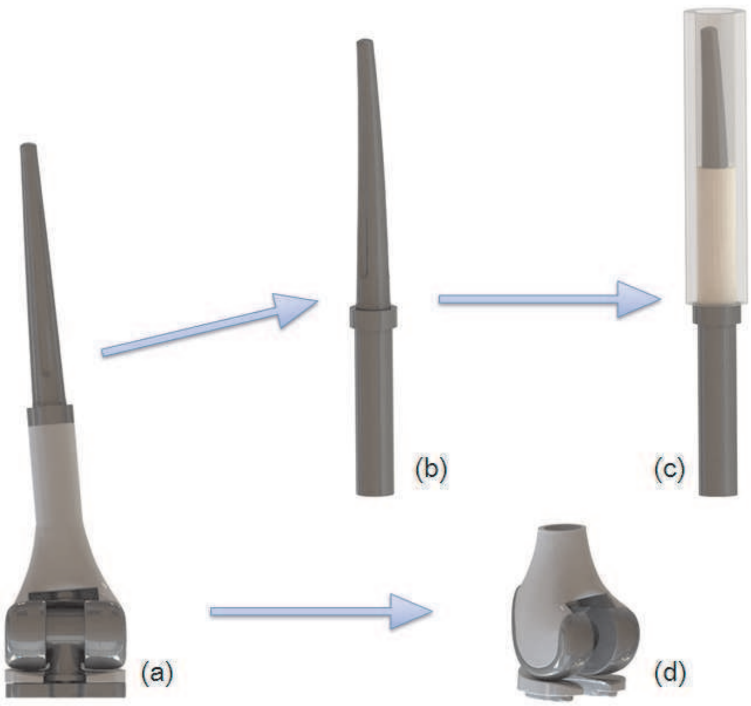

Fig. 4. 3D model of knee tumor prosthesis: (a) whole tumor prosthesis, (b) femoral stem, (c) femoral stem with femur and bone cement, (d) femoral condyle and tibial plateau.

the collision on the UHMWPE femoral component and the tibial plateau, a tibiofemoral contact model was developed as shown in Fig 4 (d). And an upper components model was separated from the whole model as shown in Fig 4 (c) for the purpose of finding out the effect of the misalignment angle on the stress/strain of the bone.

2.3. *FEA model*

Three dimensional finite element models were created including a tibio-femoral model and an upper components model. All the materials were modelled as homogeneous, isotropic and liner elastic, except the UHMWPE which was modelled as non-linear elastic-plastic based on the true stress-strain constitutive relationship presented in Fig 5,[21–23] and all other material properties used in this study are given in Table 1.

Table 1. Material properties used in present study.[18, 22, 24]

Component	Materials	Young's modulus (GPa)	Poisson's ratio
Tibia plateau	UHMWPE	0.463	0.46
UHMWPE femoral component	UHMWPE	0.463	0.46
Femoral condylar	Titanium alloy	110	0.35
Femoral stem	Titanium alloy	110	0.35
Bone cement	PMMA	2.5	0.25
Femur	Cortical bone	11.5	0.30

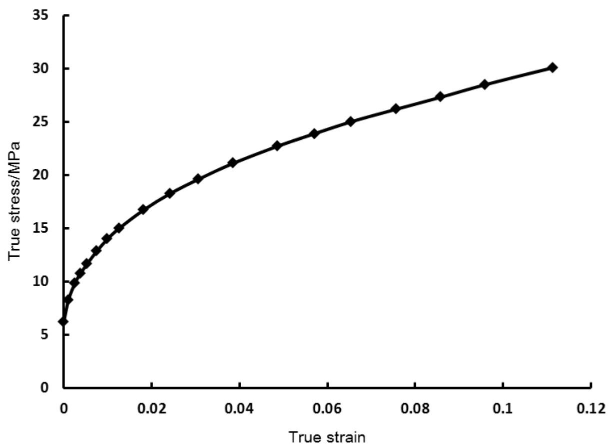

Fig. 5. Non-linear true stress-strain UHMWPE material model.

2.3.1. *Tibio-femoral analysis*

A simplified solid model which included the UHMWPE femoral component, the UHMWPE tibia plateau and the titanium alloy femoral condyle was imported to ABAQUS/CAE (Dassault, France) from Solidworks (Dassault, France). The titanium alloy femoral condyle was defined as rigid in the contact analysis since it has a much higher Young's modulus value compared with other components. Boundary conditions were applied to the model to imitate squatting when the flexion-extension angle reached approximately 135° as shown in Fig 6. All the six degrees of freedom of the bottom of the tibia plateau were limited. The translation along three coordinate axes and the rotation around the Z axis (the varus-valgus degrees of freedom of both the UHMWPE femoral component and the titanium alloy femoral condyle) were restricted, too. Relative motion between the UHMWPE femoral component and the titanium alloy femoral condyle was not allowed. A torque of 15 Nm, corresponding to the torque that the knee joint suffered under squatting, was estimated from a simple statics analysis[25] and applied to the rigid body femoral condyle around the flexion-extension axis of the prosthesis. Element type for the UHMWPE femoral component, the UHMWPE tibia plateau and the titanium alloy femoral condyle were chosen as C3D10M (a 10-node modified quadratic tetrahedron element) on account of its high accuracy and excellent performance in contact analysis. Mesh sensitivity was conducted, and a meshing size of 2 mm was found to be accurate enough as the relative error between meshing size of 2 mm and 1 mm was below 5%. The element number of the titanium alloy femoral condyle was 84701 and 63127 for the UHMWPE femoral component while the element number of the tibial plateau was 51051. Contact surface was defined as shown in Fig 6 to calculate the contact pressure when the collision between the UHMWPE femoral component and the UHMWPE tibia plateau occurred.

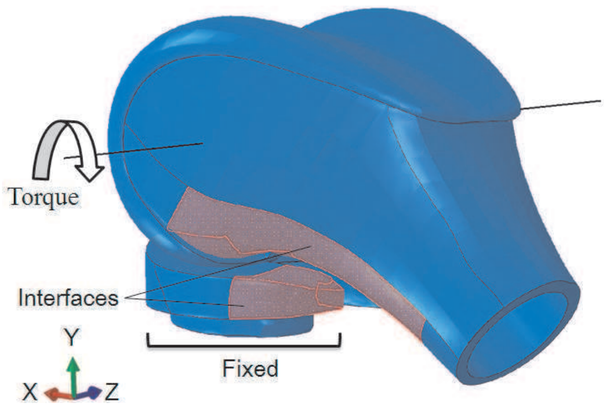

Fig. 6. FE model of tibio-femoral joint.

2.3.2. *Femoral stem analysis*

Another solid model included the femoral stem, a simplified femur which the thickness was 5 mm and the bone cement was developed in ABAQUS/CAE. The femoral stem was defined as rigid body. As shown in Fig 7 (a), the interface between the bone cement and the intramedullary nail was tied, which was same to the interface between the femur and the bone cement. The lower part of the femoral stem was fully constrained. A pressure of 5.305 MPa corresponding to a concentrate force of 2600 N, approximately equaling to 4 times body weight for the patient's weight of 69 kg, was applied on the top surface of the simplified femur as shown in Fig 7 (a). For the purpose of the investigation of the effect of misalignment angle and direction on the stress in the bone, misalignment angles between the anatomical axis of the femur and the axis of the femoral stem were defined as 3° and 6°, respectively. As 3° is within the normal clinical error in arthroplasty[26] while 6° was chosen to study the consequence of an unsatisfactory surgery. The

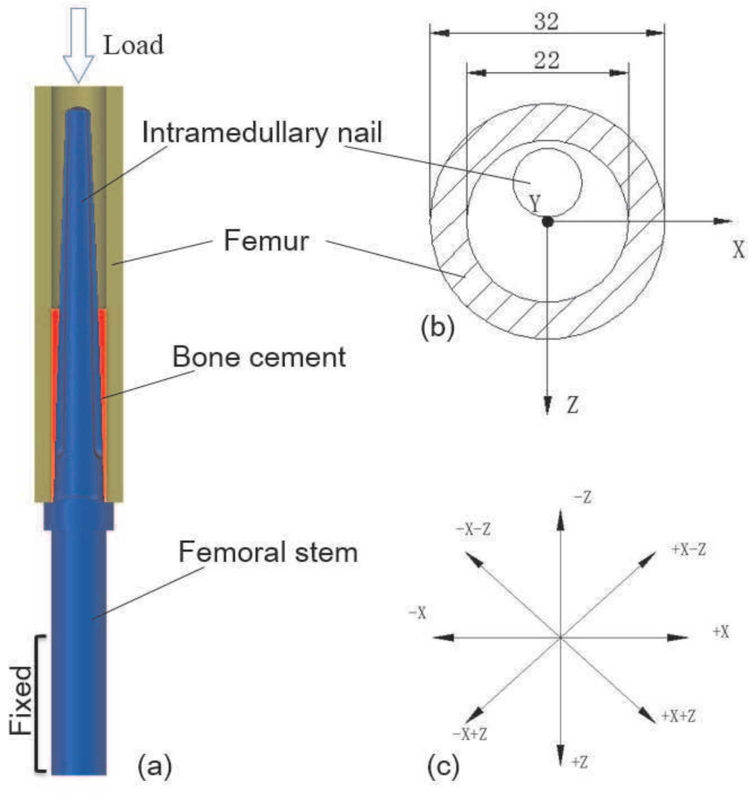

Fig. 7. (a) FE model of femoral stem, bone cement and femur. (b) The cross section of the model. (c) The illustration of misalignment direction.

misalignment direction was defined in Fig 7 (b) and (c): X was considered to be positive in the medial to lateral direction while Z was considered to be positive from posterior to anterior. Eight equally spaced misalignment directions were considered. Element type for the femoral stem, the femur and the bone cement was chosen as C3D10M and meshing size was 2 mm, which were same as the tibio-femoral contact analysis. The number of element of the femoral stem, femur and bone cement was 62435, 55522 and 17062, respectively.

3. Results

3.1. *Tibio-femoral analysis*

The collision between the tibial plateau and the UHMWPE femoral component was simulated using FEA modeling. The maximum contact pressure on the surface of the tibial plateau was 44.88 MPa at the lateral part and the maximum contact pressure at the medial tibial plateau was 36.62 MPa. The estimated von Mises stress at the tibial plateau showed a large stress concentration near the interface between the tibial plateau and the UHMWPE femoral component. The maximum von Mises stress at the tibial plateau was 33.79 MPa at the medial plateau while at the lateral plateau was 31.22MPa. The estimated von Mises stress and contact pressure are presented in Fig 8.

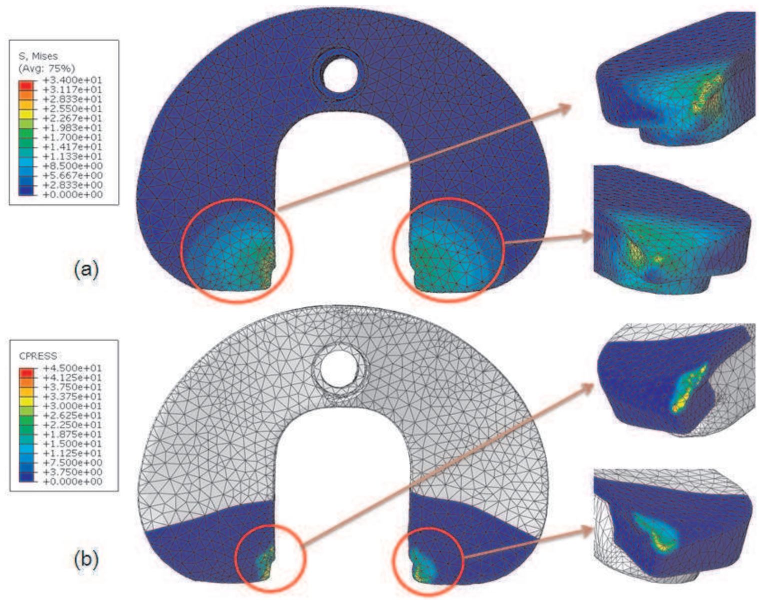

Fig. 8. The contour plot of the predicted (a) von Mises stresses and (b) contact pressure (MPa) at the tibial plateau.

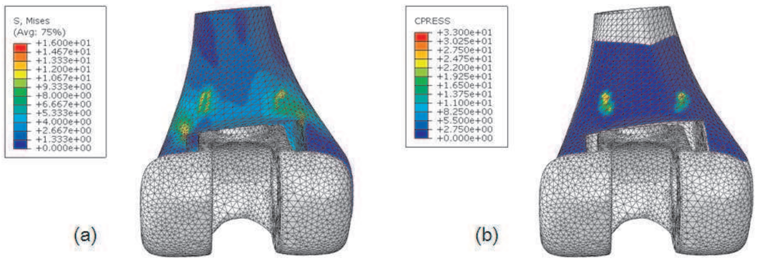

Fig. 9. The contour plot of the predicted (a) von Mises stresses and (b) contact pressure (MPa) at the UHMWPE femoral component.

In addition, von Mises stress and contact pressure at the UHMWPE femoral component were calculated and are presented in Fig 9. The local maximum von Mises stress was 15.58 MPa around the interface between the UHMWPE femoral component and the tibial plateau.

3.2. *Femoral stem analysis*

The maximum von Mises stress together with the maximum deformation were predicted when the femur stem was at misalignment angles of 3 $^\circ$ and 6 $^\circ$ away from anatomical axis of the femur and are presented in Table 2. The predicted von Mises stress and strain distribution at the femur at a misalignment angle of 6 $^\circ$, in the positive Z axis direction of are presented in Fig 10 as an example. The maximum von Mises stress appeared on the same side of misalignment direction (see Fig 10 (a) left) near the middle section of the femur while the maximum deformation appeared at the proximal femur. And the comparison of these two groups is presented in Fig 11.

Table 2. Maximum von Mises stress and maximum deformation at femur when the misalignment angle was 3 $^\circ$ and 6 $^\circ$.

Tilting angle/ $^\circ$	3		6	
Tilting direction	Maximum Mises stress (MPa)	Maximum deformation (mm)	Maximum Mises stress (MPa)	Maximum deformation (mm)
+Z	9.78	0.592	12.97	1.166
-Z	10.38	0.590	12.81	1.164
+X	10.27	0.591	12.87	1.164
-X	10.29	0.589	12.84	1.161
+X,+Z	10.02	0.590	12.89	1.169
+X,-Z	10.53	0.591	13.03	1.172
-X,+Z	9.76	0.591	12.92	1.172
-X,-Z	10.80	0.586	13.37	1.165

4. Discussion

In this study, the retrieved custom-made knee prosthesis was analysed by three dimensional finite element method. From the observation of the retrieval prosthesis, serious deformation and wear were found at the posterior region of the tibial plateau. And the collision between the UHMWPE femoral component and the tibial plateau was speculated as the main cause of it. More specially, the collision happened under the flexion angle of 135 ° from the tibio-femoral contact analysis while large values

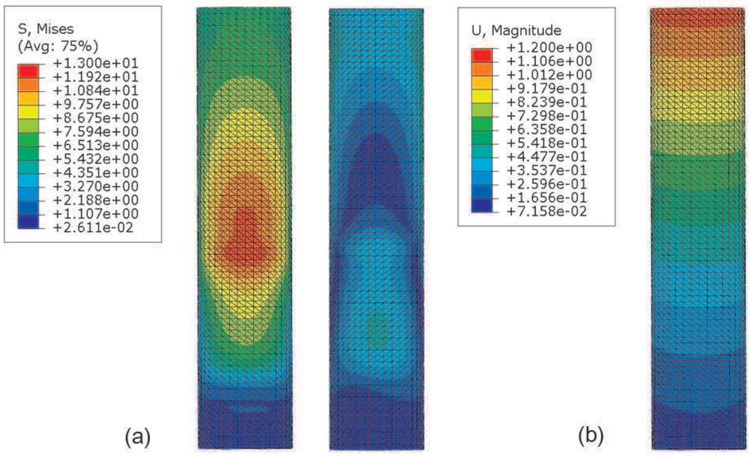

Fig. 10. The predicted von Mises stress (MPa) and deformation (mm) distribution at the femur when the misalignment angle was 6 ° in the Z direction.

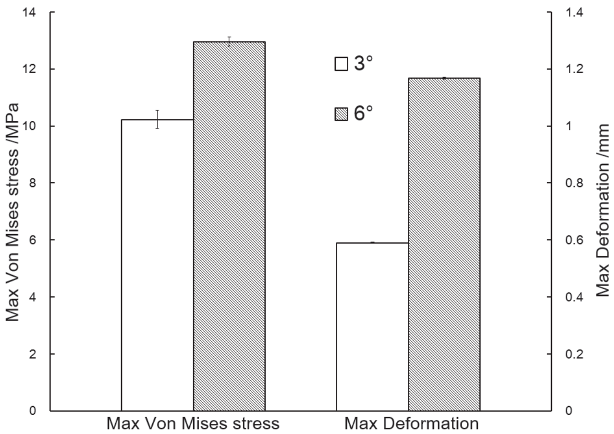

Fig. 11. The Maximum Von Mises stress and maximum deformation at the femur when misalignment angle was 3 ° and 6 ° respectively (error bar stands for standard deviation for eight directions).

of von Mises stress and contact pressure were found near the contact region between them. The close observation of the surface revealed a number of features as shown in Fig 3 (b). The worn surface morphology of the posterior region at the tibial plateau indicated wear mechanism including the scratching, the abrasion and the permanent deformation which related to the complex relative movement between the tibial plateau and the UHMWPE femoral component when the knee was under deep flexion during squatting or kneeling.

A great deal of material loss was found at the posterior region of the tibial plateau, corresponding to the high contact pressure area from the computational prediction. Fatigue wear occurred at the tibial plateau as it was under alternate loading which was much larger than the compressive yield stress of UHMWPE over a long period of time. The compressive yield stress of UHMWPE was 15-20 MPa in general.[27,28]Taking into account the impact of the relative sliding on the interface between the tibial plateau and the UHMWPE femoral component, a mass of material loss at the posterior region of the tibial plateau was produced. And then, wear debris, primary generated from the material loss of the UHMWPE components, would induce adverse biological response that leads to osteolysis and aseptic loosening.[29–32] Most Asian population had the habit of squatting or kneeling which would cause the collision between the tibial plateau and the UHMWPE femoral component. The collision would have caused great shock or stress on both tibial and femoral components. Furthermore, the proximal femoral prosthesis was lack of bony support.[33] Hence, the femoral stem had to bear bending moment which came from the collision. Besides, great von Mises stress was applied to the intramedullary nail and the femoral stem of the prosthesis by the collision. Structural improvement and optimization or a reasonable selection of the custom-made knee prosthesis should be considered to avoid the collision when the joint was under fairly high flexion-extension angle. Proper clinical postoperative guidance[34] such as minimizing times and duration of squatting or kneeling of patients in postoperative training programme should be encouraged to lower the occurrence of the collision.

From the result in the femoral stem analysis, the maximum von Mises stress and deformation at the femur was about 10 MPa and 0.6 mm respectively when the misalignment angle between the anatomical axis of the femur and the axis of the femoral stem of 3°. Since the misalignment angle of 3° was considered to be acceptable,[26] it was chosen as the control in this study. However, it was generally thought that the 0.5 mm deformation was the maximum deformation allowed on the cortical bone.[35–37] That is, even a successful operation may cause a large value of strain out of tolerance at the femur, which means a more accurate surgical positioning is required. . The maximum von Mises stress on the femur increased by about 25% when the misalignment angle was 6° while the maximum deformation under 6° was almost doubled. It is clear that both von Mises stress and deformation at the femur increased dramatically with the increased misalignment. It would lead to uneven stress distribution within the femur.Specially, take the stress distribution at the femur when the misalignment was 6° in the Z direction as an example, as presented in Fig 10 (a) (right), the stress value is below 7 MPa at "-Z" side of the bone. This part of bone experienced a lower stress and consequently resulted in stress shielding and aseptic loosening.[38, 39] The aseptic loosening further exacerbated the misalignment between the anatomical axis of the femur and the axis of the femoral stem. The increase of the misalignment angle, as evident from the CT image in Fig 1 (b), confirmed this viewpoint. In addition, the intramedullary nail was designed to fill the intramedullary space, and a relatively large diameter was chosen. This further accelerated the stress shielding.

This study had several limitations, most due to the model simplification. First, a simplified hollow cylinder femur model was used in the finite element analysis. Second, simplified loading conditions were applied, with only the axial force and the torque caused by the axial force considered in the finite element model but other forces and torques such as the internal-external force and the varus-valgus torque applied at the prosthesis in body were ignored which may have led to some errors.

5. Conclusions

A retrieval study on a custom-made knee prosthesis was carried out by three dimensional finite element analysis. The failure reasons were investigated from a mechanical perspective. The analysis performed in this case indicated three factors that might cause the failure of the prosthesis. Firstly, the prosthetic design or selection was unreasonable. An applicable selection of the prosthesis should give the consideration to the living habit of the patient. Secondly, the misalignment between the femoral stem and the anatomical axis of the femur would generate stress shielding and aseptic loosening due to component misalignment. Thirdly, the habit of squatting or kneeling caused impingement between the posterior region of the UHMWPE tibia plateau and the UHMWPE femoral component led to a great deal of material loss and indirectly exacerbated aseptic loosening.

6. Acknowledgements

This work was supported by the Program of the National Natural Science Foundation of China [51205303] and [51323007], National Science and Technology Supporting Program [2012BAI18B00].

References

1. Orlic D, Smerdelj M, Kolundzic R, Bergovec M, Lower limb salvage surgery: modular endoprosthesis in bone tumour treatment, *Int Orthop* **30**:458–464, 2006.
2. Ahlmann E, Menendez L, Kermani C, Gotha H, Survivorship and clinical outcome of modular endoprosthetic reconstruction for neoplastic disease of the lower limb, *J Bone Joint Surg BR* **88**:790–795, 2006.

3. Jeys L, Kulkarni A, Grimer R, Carter S, Tillman R, Abudu A, Endoprosthetic reconstruction for the treatment of musculoskeletal tumors of the appendicular skeleton and pelvis, *J Bone Joint Surg* **90**:1265–1271, 2008.
4. Balke M, Ahrens H, Streitbürger A, Hardes J, *Modular endoprosthetic reconstruction in malignant bone tumors: indications and limits*, Springer, Berlin Heidelberg, 2009.
5. Blunn GW, Joshi AB, Minns RJ, Lidgren L, Lilley P, Ryd L, et al, Wear in retrieved condylar knee arthroplasties: A comparison of wear in different designs of 280 retrieved condylar knee prostheses, *J Arthroplasty* **12**:281–290, 1997.
6. Galasso O, Mariconda M, Brando A, Iannò B, Disassembly of a Distal Femur Modular Prosthesis After Tumor Resection, *J Arthroplasty* **25**:334.e5–e9, 2010.
7. Oliveira ALL, Cueva EG, Carvalho RT, Failure analysis of the tibial component baseplate after total knee arthroplasty, *Eng Fail Anal* **36**:147–154, 2014.
8. Chao J, Lòpez V, Failure analysis of a Ti6Al4V cementless HIP prosthesis, *Eng Fail Anal* **14**:822–830, 2007.
9. Hernandez-Rodriguez MAL, Ortega-Saenz JA, Contreras-Hernandez GR, Failure analysis of a total hip prosthesis implanted in active patient, *J Mech Behav Biomed Mater* **3**:619–622, 2010.
10. Roffey P, Case study: Failure of a high nitrogen stainless steel femoral stem, *Eng Fail Anal* **20**:173–183, 2012.
11. Liza S, Haseeb ASMA, Abbas AA, Masjuki HH, Failure analysis of retrieved UHMWPE tibial insert in total knee replacement, *Eng Fail Anal* **18**:1415–1423, 2011.
12. Gitelis S, Yergler JD, Sawlani N, Schiff A, Shott S, Short-and Long-term Failure of Modular Oncology Knee Prostheses, *Orthopedics* **31**:362, 2008.
13. Biau D, Faure F, Katsahian S, Jeanrot C, Tomeno B, Anract P, Survival of total knee replacement with a megaprosthesis after bone tumor resection, *J Bone Joint Surg* **88**:1285–1293, 2006.
14. Godest A, Beaugonin M, Haug E, Taylor M, Gregson P, Simulation of a knee joint replacement during a gait cycle using explicit finite element analysis, *J Biomech* **35**:267–275, 2002.
15. Halloran JP, Petrella AJ, Rullkoetter PJ, Explicit finite element modeling of total knee replacement mechanics, *J Biomech* **38**:323–311, 2005.
16. Abdelgaied A, Liu F, Brockett C, Jennings L, Fisher J, Jin Z, Computational wear prediction of artificial knee joints based on a new wear law and formulation, *J Biomech* **44**:1108–1116, 2011.
17. Knight LA, Pal S, Coleman JC, Bronson F, Haider H, Levine DL, et al, Comparison of long-term numerical and experimental total knee replacement wear during simulated gait loading, *J Biomech* **40**:1550–1558, 2007.
18. Chong DY, Hansen UN, Amis AA, Analysis of bone-prosthesis interface micromotion for cementless tibial prosthesis fixation and the influence of loading conditions, *J Biomech* **43**:1074–1080, 2010.
19. Griza S, dos Santos SV, Ueki MM, Bertoni F, Strohaecker TR, Case study and analysis of a fatigue failure in a THA stem, *Eng Fail Anal* **28**:166–175, 2013.
20. Fonseca F, Rebelo E, Completo A, Tibial periprosthetic fracture combined with tibial stem stress fracture from total knee arthroplasty, *Rev Bras Ortop* **46**:745–750, 2011.
21. Liu F, Contact mechanics and elastohydrodynamic lubrication analysis of metal-on-metal hip implant with a sandwich acetabular cup under transient walking condition, Ph.D. Thesis, Leeds University, 2005.
22. Hua X, Wroblewski BM, Jin Z, Wang L, The effect of cup inclination and wear on the contact mechanics and cement fixation for ultra high molecular weight polyethylene total hip replacements, *Med Eng Phys* **34**:318–325, 2012.

23. Liu F, Galvin A, Jin Z, Fisher J, A new formulation for the prediction of polyethylene wear in artificial hip joints, *P I MECH ENG H* **225**:16–24, 2011.
24. Fregly BJ, Bei Y, Sylvester ME, Experimental evaluation of an elastic foundation model to predict contact pressures in knee replacements, *J Biomech* **36**:1659–1668, 2003.
25. Komistek RD, Kane TR, Mahfouz M, Ochoa JA, Dennis DA, Knee mechanics: a review of past and present techniques to determine in vivo loads, *J Biomech* **38**:215–228, 2005.
26. Stulberg SD, How accurate is current TKR instrumentation? Clinical orthopaedics and related research, *Clin Orthop Relat Res* **416**:177–184, 2003.
27. Takeuchi T, Lathi V K, Khan A M, W C Wilson, Patellofemoral contact pressures exceed the compressive yield strength of UHMWPE in total knee arthroplasties, *J Arthroplasty* **10**:363–368, 1995.
28. Kuster M S, Wood G A, Stachowiak G W, Joint load considerations in total knee replacement, *J Bone Joint Surg BR* **79**:109–113, 1997.
29. Xiong D, Gao Z, Jin Z, Friction and wear properties of UHMWPE against ion implanted titanium alloy, *Surf Coat Technol* **201**:6874–6850, 2007.
30. Wirth MA, Agrawal CM, Mabrey JD, Dean DD, Blanchard CR, Miller MA, et al, Isolation and Characterization of Polyethylene Wear Debris Associated with Osteolysis Following Total Shoulder Arthroplasty, *J Bone Joint Surg* **81**:29–37, 1999.
31. Urban RM, Jacobs JJ, Tomlinson MJ, Gavrilovic J, Black J, Peoc'h M, Dissemination of Wear Particles to the Liver, Spleen, and Abdominal Lymph Nodes of Patients with Hip or Knee Replacement, *J Bone Joint Surg* **82**:457, 2000.
32. Unwin P, Cannon S, Grimer R, Kemp H, Sneath R, Walker P, Aseptic loosening in cemented custom-made prosthetic replacements for bone tumours of the lower limb, *J Bone Joint Surg BR* **78**:5–13, 1996.
33. Kaste SC, Neel MD, Meyer WH, Pratt CB, Rao BN, Extracortical bridging callus after limb salvage surgery about the knee, *Clin Orthop Relat Res* **363**:180–185, 1999.
34. Okita Y, Tatematsu N, Nagai K, Nakayama T, Nakamata T, Okamoto T, et al, Compensation by nonoperated joints in the lower limbs during walking after endoprosthetic knee replacement following bone tumor resection, *Clin Biomech* **28**:898–903, 2013.
35. Carter DR, Mechanical loading histories and cortical bone remodeling, *Calcif Tissue Int* **36**:S19–S24, 1984.
36. Burr DB, Milgrom C, Fyhrie D, Forwood M, Nyska M, Finestone A, et al, In vivo measurement of human tibial strains during vigorous activity, *Bone* **18**:405–410, 1996.
37. Courtney AC, Hayes WC, Gibson LJ, Age-related differences in post-yield damage in human cortical bone. Experiment and model, *J Biomech* **29**:1463–1471, 1996.
38. Chong DY, Hansen UN, Amis AA, The influence of tibial prosthesis design features on stresses related to aseptic loosening and stress shielding, *J Mech Med Biol* **11**:55–72, 2011.
39. Amarasinghe R, Rupasinghe R, Anurathan P, Herath S, Effects of geometry of the intramedullary stem of the ulna component of hinged elbow joint prostheses on the bone and implant bending stresses, *J Mech Med Biol* **11**:1271–1293, 2011.